Two-terminal conductance fluctuations in the integer quantum Hall regime

Chang-Ming Ho*

Theoretical Physics, University of Oxford, 1 Keble Road, Oxford OX1 3NP, United Kingdom
(Received 15 March 1999)

Motivated by recent experiments on the conductance fluctuations in mesoscopic integer quantum Hall systems, we consider a model in which the Coulomb interactions are incorporated into the picture of edge-state transport through a single saddle point. The occupancies of *classical* localized states in the two-dimensional electron system change due to the interactions between electrons when the gate voltage on top of the device is varied. The electrostatic potential between the localized states and the saddle point causes fluctuations of the saddle-point potential and thus fluctuations of the transmission probability of edge states. This simple model is studied numerically and compared with the observation. [S0163-1829(99)11835-6]

I. INTRODUCTION

Mesoscopic sample-to-sample fluctuations in the conductance G are universal in the sense that the deviation from its average, $(\delta G)^2 = (G - \langle G \rangle)^2$, is always about the order of $(e^2/h)^2$ at very low temperature.[1,2] In zero or weak external magnetic fields, this behavior can be understood in terms of the quantum phase coherence of diffusive electrons.[3] This picture, however, is not expected to work in the quantum Hall regime since the trajectories of electrons are drastically deformed in strong magnetic fields. In this situation, the existence of extended states at sample edges makes the transport properties rather different from the weak-field case.[4] Indeed, magnetoconductance measurements on mesoscopic multiterminal devices[5–8] seem to agree with this expectation. To be consistent with these observations, explicit inclusion of the edge-channel effects in theories seems to be necessary.[9–11]

The appearance of the bulk delocalized states when the Fermi level is between two quantized Hall plateaus makes a mesoscopic system in strong magnetic field even more interesting.[12] It is only recently, however, that experimental data on the statistical behavior of the conductance in this regime have become available.[13] Specifically, conductance fluctuations have been studied in mesoscopic n-channel silicon metal-oxide-semiconductor field-effect transistors[14] (Si MOSFETs) with two terminals. In these systems, conductance is quantized (in units of e^2/h) at some values of the gate voltage V_g and the complication due to the Shubnikov–de Haas oscillation in multiterminal devices is absent in the two-terminal setting. It is found that the distribution of conductance below the first conductance plateau is almost uniform between $G = 0$ and e^2/h. This is in clear contrast to the Gaussian distribution in the weak-field case.[13] Theoretical studies have been carried out on models based on the single-particle interference effect, e.g., the tight-binding Hamiltonian,[15] Chalker-Coddington network model,[16–18] and so on[19] numerically, and also a renormalization group analysis.[20] Some capture this feature of the conductance distribution.

More recently, Cobden and collaborators demonstrate further that there is a great difference between conductance fluctuations in the lowest few Landau levels and the weak-field case.[21,22] Using the same sets of Si MOSFET devices as described, they observed in strong fields strong correlations of fluctuation peaks and dips at different magnetic fields. This is achieved by studying explicitly the evolution of fluctuation peaks and dips with magnetic fields in different field regimes. Using a gray scale plot of dG/dV_g as a function of B and V_g, each bright or dark line can be viewed as the "history" line of a peak or a dip of the conductance at different combinations of V_g and B. The contrast between weak and strong magnetic fields is very clear (see Fig. 2 in Ref. 21).

For weak magnetic fields, no pattern can be seen whatsoever. At $B \gtrsim 10$ T, we can see peaks and dips of conductance fluctuations in a transition region between two successive conductance plateaus, which are wide and gray regions. The fluctuations "move" in gate voltage, in straight lines as the magnetic field is varied. This pattern means that there exist strong correlations between fluctuation peaks and dips at different gate voltages at high magnetic fields. A closer look reveals that there are two types of lines, with different slopes, in a transition region. The slope of one set of lines is parallel to that associated with the center of the plateau below, while the slope of the other set of lines is parallel to that associated with the center of the plateau above.

The strong contrast between the fluctuations on the V_g-B plots in weak and strong magnetic fields means that what occurs in two different field regimes is dramatically different. The straight lines appearing in the strong-field results make it no longer appropriate to treat the phenomenon as a single-particle one. Thus those models[15–20] we mentioned before are obviously not compatible with strong correlations of conductance fluctuations at different fields.

In this paper, we consider a model taking into account the electron-electron interactions. The conductance plateaus are understood in terms of the edge-state picture and the absence of backscattering between channels at opposite edges of the sample. In the transition region between plateaus, we assume that the paths followed by electron currents coming from two contacts (or terminals) percolate into the bulk as the chemical potential is increased and eventually become connected by tunneling through a single saddle point. In addition to the electrons in these edge states, we also take account of electrons in localized states. Conductance fluctuations arising

from Coulomb interactions between both sets of electrons are treated in a simple way.

As electrons are added to the system, the ones already in the localized states will rearrange due to the interactions. Therefore, the occupation of a given localized state can fluctuate several times between 0 and 1 when the chemical potential μ is changed from $-\infty$ to $+\infty$. The total electrostatic potential between the localized states and the saddle point then also fluctuates as μ is varied. Because of the fluctuations of the saddle-point potential, the tunneling of percolation paths fluctuates as a function of the chemical potential. In our model, fluctuations of the conductance are purely due to these interaction effects. Numerical study of this model shows that the conductance between plateaus as a function of the chemical potential does indeed fluctuate significantly within the range between $G=0$ and e^2/h.

In the next section, we first develop our model, based on the transmission of edge-state channels through a single saddle point in the transition region. Fluctuations of a single potential saddle point are related to the Coulomb interaction between localized states in the bulk of the disordered two-dimensional electron system (2DES). These localized states are treated using the Efros-Shklovskii Coulomb glass model. Models at finite temperature T with localized states arranged on regular lattice points or random sites are then studied numerically by Monte Carlo methods and exact enumeration. Results for G versus V_g at different disorder configurations and temperatures are obtained. After that, comparisons of our numerical results and experiments are discussed. We conclude with a summary.

II. THEORETICAL MODEL

Before introducing the model, we note that there are different electron states in a disordered 2DES system in a high magnetic field. The edge state exists on an equienergy line along the boundary of the sample connecting two contacts. The width of each edge-state channel is about the order of magnetic length, $l_B \propto 1/\sqrt{B}$. Therefore, in a high magnetic field the backscattering between edge states at opposite boundaries can be neglected. Since each of the edge-state channels is now one dimensional, we can apply the two-terminal Landauer-Büttiker formula to calculate the conductance. The current injected into each of the edge states is proportional to the difference of chemical potentials between two contacts and also each edge-channel pair. In the context of the measurements on Si MOSFETs,[13,21,22] the bias voltage between two contacts is fixed, but the gate voltage of the metallic gate on top of the 2DES, therefore the Fermi energy, is varied. As the number of electrons is increased such that the Fermi level is between Landau levels $E_n < E_F < E_{n+1}$, there are n edge channels at each boundary. In a high magnetic field with no interedge backscattering, the conductance of the system is thus quantized and given by $G=ne^2/h$.

In the transition region between two quantized plateaus, it is clear that the Fermi level is within a disorder-broadened Landau level. For clarity, let us consider what happens when the conductance is between the first and the second plateaus (see Fig. 1). At zero temperature, there are localized states in the bulk associated with closed local equipotential lines,[12] shown as dashed and dotted closed lines in Fig. 1. Apart
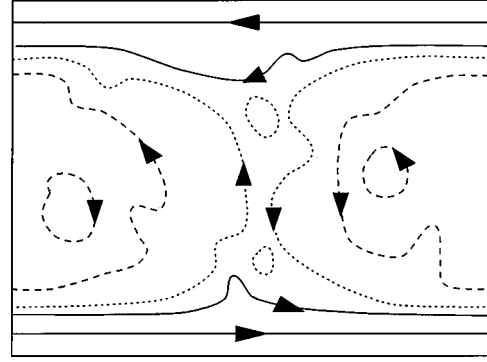

FIG. 1. The formation of an edge-state channel pair as the gate voltage is increased in the transition regime, here between $G=e^2/h$ and $2e^2/h$. The lines with arrows represent the directed trajectories of electrons or holes in the magnetic fields.

from them, we can imagine that, in the bulk of the system, there are also directed extended states at the boundaries of the regions which are occupied by electrons and connected to one or the other contact. At some value of the chemical potential, these extended states undergo large excursions into the bulk. As μ is increased further, the directed extended states approach each other more closely and tunneling between them occurs (shown as the dotted line in Fig. 1). Eventually, a second pair of edge states is formed in this way at the inner side near the system boundaries.

Let us consider the simplest tunneling process in which the two growing regions of electrons form a single potential saddle point assumed to be located at about the center of the 2DES. The transmission probability $T_{ij}=|t_{ij}|^2$ for the incoming channel i and outgoing channel j is already known, for the saddle-point potential of the form $V(x,y)=V_0-(1/2)m\omega_x^2 x^2+(1/2)m\omega_y^2 y^2$ with ω_x and ω_y characterizing the shape of the saddle-point potential.[23] It is given by

$$T_{ij} = \delta_{ij} \frac{1}{1+\exp(-\pi\epsilon_n)}, \tag{1}$$

where $\epsilon_n = [E - E_2(n+1/2) - V_{SP}]/E_1$ with E denoting the total energy of the electron and $V_{SP}=V_0$ being the bare potential strength. The two-terminal conductance is then given by $G=(e^2/h)\Sigma_i T_{ii}$.

In Eq. (1), E_1 and E_2 are in general complicated functions of ω_c (cyclotron frequency), ω_x, and ω_y. At high magnetic fields, when ω_c is much bigger than ω_x and ω_y, ϵ_n in Eq. (1) is simply a dimensionless measure of the energy of the electron's guiding-center motion relative to V_0. For the edge state of the percolating region with a guiding-center energy $E_G=E_F-\hbar\omega_c(n+1/2)$, the transmission probability is 1 if $E_G \gg V_0$. In the other limit that $E_G \ll V_0$, the edge state is completely reflected. The two-terminal conductance as a function of Fermi energy at various magnetic-field strengths has been obtained numerically by Büttiker.[24] Interestingly, although these results are for a 2DES with a point-contact constriction or split gates on top, the same structure is observed in a ''macroscopic'' Si MOSFET.[22] From this, it seems that considering only one potential saddle point in the mesoscopic Si MOSFET where measurements were carried out may be reasonable.

Within the framework of the edge-state picture described above, fluctuations of the transmission of percolating states lead to the conductance fluctuations. Here the transmission of electron currents depends solely on the potential energy at the saddle point. In general, this potential energy should have a contribution from the interactions. It is our purpose to relate the interactions to the conductance fluctuations. Electrons in our model are separated into categories: those in edge states and those in localized states. In principle, a full treatment of two interactions between electrons is very complicated.[25] For simplicity, we neglect interactions among electrons in edge states, and just consider interactions between different electrons in localized states and their effect on the saddle-point potential. Equally, for simplicity, we neglect tunneling processes that mix the states we term localized with each other or with those we term edge states. This is correct in a finite sample in the semiclassical limit, when for a given value of the Fermi energy tunneling is important only at one saddle point of the potential. More generally, one expects states at the plateau transition to be delocalized by the tunneling processes we omit, at least within a single-particle description. Note that, although interactions between extended electrons are left completely untreated in the model, it turns out, as we shall present later, that this way of including the Coulomb interaction does indeed produce dramatic fluctuations of the saddle-point potential as the chemical potential of the system is varied.

The model Hamiltonian describing a system of localized states interacting with the Coulomb interaction is essentially the one which was studied first by Efros and Shklovskii.[26] The same Hamiltonian produces a gap in the single-electron density of states at the Fermi level due to the Coulomb interaction. In the ''Coulomb-gap'' system, electrons are strongly localized on a discrete set of sites due to the impurities. These quantum particles can thus be thought of as being in the regime where they behave classically. The Hamiltonian for localized states on N sites at positions denoted by i is

$$H = \sum_{i=1}^{N} \epsilon_i \left(n_i - \frac{1}{2} \right) + \frac{1}{2} \sum_{i \neq j}^{N} \frac{e^2}{4\pi\varepsilon\varepsilon_0} \frac{\left(n_i - \frac{1}{2} \right)\left(n_j - \frac{1}{2} \right)}{r_{ij}}$$
$$- \mu \sum_{i=1}^{N} \left(n_i - \frac{1}{2} \right), \qquad (2)$$

where ϵ_i is the random site energy, n_i is the occupation number which can be either 0 or 1, and r_{ij} is the distance between sites i and j. The subtraction of $1/2$ from n_i represents neutralizing background charge. ε and ε_0 are dielectric constants for the silicon and the vacuum, respectively. The last term in the Hamiltonian is crucial to model the experimental variation in the chemical potential in the system as the gate voltage is varied. More explicitly, as the voltage of the gate electrode on top of the 2DES is varied, there will be electrons brought in or pulled out of the 2DES in the inversion layer in the silicon. The occupancy in each of the localized states will then fluctuate as a function of μ, due to the Coulomb interaction. Accordingly, the electrostatic poten-

tials between the N localized states and the saddle-point potential will also fluctuate. Hence we have a fluctuating total saddle-point potential

$$V_{SP} = \sum_{i}^{N} \frac{e^2}{4\pi\varepsilon\varepsilon_0} \frac{\left(n_i - \frac{1}{2} \right)}{\sqrt{r_{i,SP}^2 + h^2}} - V_0, \qquad (3)$$

with $r_{i,SP}$ representing the distance between site i and the saddle point, where h is the perpendicular distance between the inversion layer containing localized states and the center of the saddle point. Again, the occupation at site i is given by $(n_i - 1/2)$ to take into account background charges. Note that at finite temperature T, in Eq. (3) we need the thermal average of the occupation number, $\langle n_i \rangle$, instead of n_i at each site i. As a result, the transmission probability given by Eq. (1) fluctuates as a function of the gate voltage.

III. NUMERICAL RESULTS AND COMPARISONS WITH EXPERIMENTS

In this section, we present the results obtained numerically at finite temperature. The 2DES is chosen to have a rectangular shape with length L and width W in units of lattice spacing. The localized states are chosen to be fixed at sites i arranged on a regular lattice with positions given by (x,y). At fixed temperature T, we compute $\langle n(x,y) \rangle$, at each site i with coordinates (x,y) for each chemical potential μ. Note that, here and in all the following computation, we have set the electric charge $4\pi\varepsilon\varepsilon_0$ and the Boltzmann constant k_B to be 1. For each configuration of impurities, a random energy is attached to each localized state. The random site energy ϵ_i at site i is some value in the interval $[-\mathcal{W}/2, \mathcal{W}/2]$. After $\langle n(x,y) \rangle$ is obtained, Eq. (3) determines the value of V_{SP} at this μ and temperature T. The corresponding transmission probability is then given by Eq. (1), rewritten here as $T_{ii} = 1/1 + \exp[-(V_{SP} + c)/E_0]$, where c is a constant representing the energy of the electron's guiding center (or the equipotential line);[23] c, however, is always set to be equal to V_0 in our numerical study. E_0 here is an energy scale, chosen arbitrarily, which in principle can depend on the magnetic field and the characteristics of the saddle point. The conductances at different chemical potentials are calculated in this way by employing the same set of random energies at N sites. For different sets of random site energies which essentially represent different disorder realizations, sample-to-sample fluctuations can then be compared. Numerical studies have been carried out using different thermal-averaging methods: the Metropolis Monte Carlo algorithm and exact enumeration.

Due to the probabilistic nature of the Metropolis Monte Carlo algorithm, it is important to ensure that the system has reached equilibrium, and that the Monte Carlo average indeed gives the thermal average. Due to the long-range interaction term, we expect that a large system will need an extremely long time to reach equilibrium. At higher temperature, stronger disorder (i.e., larger $\mathcal{W}$), and larger $|\mu|$, this difficulty may be avoided since the contribution of the Coulomb interaction is then small. It turns out that at low temperature fluctuations due to lack of equilibration are rather large up to the biggest (6×6) system we have
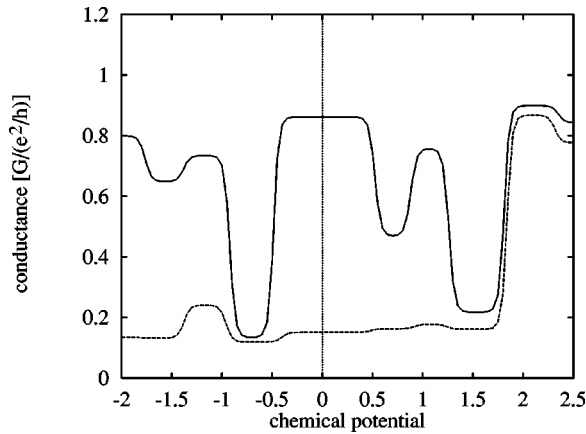
FIG. 2. Conductance versus chemical potential on a 5×4 lattice at $T=0.03$, $\mathcal{W}=0.2$, $E_0=5$, and $h=0.3$. The saddle point is chosen to be at $(x,y)=(3,2)$. Two lines are for different realizations of impurity configuration.
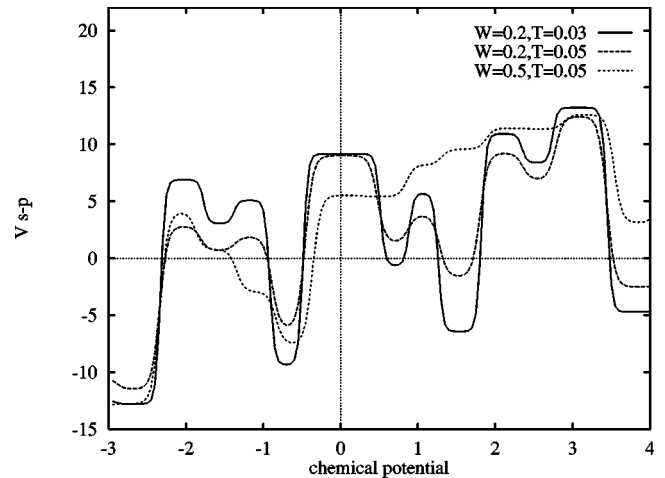

FIG. 3. Fluctuations of the saddle-point potential V_{SP} at $(x,y)=(3,2)$ versus chemical potential (or gate voltage) on 5×4 systems. $h=0.3$ for all results here.

reached. In order to study the fluctuations due to interactions in more detail, we turn to calculate the thermal average using exact enumeration. In doing so, what occurs in lower temperature can be investigated more explicitly.

Exact enumeration means that the thermal averages are achieved by finding explicitly all possible state configurations and calculating their Boltzmann factors. From the comparison of results using two different methods, it is clear that those small-amplitude fluctuations obtained in using the Monte Carlo algorithm are due to the nonequilibration, instead of the interaction.

With reasonable computing time, we obtain results for systems of sizes up to 5×4. Here, only the results for 5×4 systems are presented. Figure 2 clearly exhibits significant conductance fluctuations ranging from 0 to e^2/h as the chemical potential is varied. The amplitudes of the fluctuations, however, depend on the value of the energy scale E_0. We can choose different sequences of random numbers in the program to change the random site energy at each site on the lattice. For the same disorder strength (i.e., $\mathcal{W}$), the sample-to-sample fluctuations due to different realizations of impurities can then be studied. In the two cases shown in Fig. 2, there are large-amplitude fluctuations and the details are sample dependent.

To avoid the confusions due to the arbitrary E_0, only plots of V_{SP} versus μ, instead of G versus μ, are shown in Fig. 3 where h is the only free parameter to obtain V_{SP}. We then compare results at different disorder strengths. Fluctuations due to the Coulomb interaction should be suppressed as the strength of the disorder is increased. This is more or less consistent with what is demonstrated in Fig. 3. Finite temperature is another source in our model which can smear out the amplitudes of the fluctuations. This is because, with a fixed chemical potential, different thermal energies give different averaged occupation numbers on the same lattice site. At higher temperature, each electron gains more thermal energy on average and thus the effect of Coulomb interaction is again suppressed. The temperature dependence of the solid and dashed lines shown in Fig. 3 with the same disorder strength clearly shows this behavior.

Finally, we discuss the results on a system which contains randomly distributed localized states. This seems to be a

more realistic representation of real devices. We use the exact enumeration for the thermal averaging. The positions of the localized states are chosen independently with a uniform distribution over the system. For the same number of localized states as that in the lattice system, we conclude that finite-size effects are stronger than on the lattice. Although not shown here, results for different disorder strengths show no significant fluctuations. Comparing with the results for the lattice system, fluctuations are much smaller. In order to obtain prominent interaction-driven fluctuations off lattice, it seems possible that we need to study very large random-site systems.

We now turn to describe the comparison between the numerical results from our model on a lattice and the experiments. First, let us focus on the conductance as a function of the gate voltage at some fixed magnetic field. The conductance fluctuations produced from our model are sample dependent, and varying the saddle-point potential with chemical potential can produce conductance fluctuations between $G=0$ and e^2/h. Both of these features are consistent with what has been observed in experiments.[13,21,22] However, the fluctuation patterns are rather different for our model and the experiments. It is observed in experiments that the conductance fluctuates in sharp peaks and dips in the transition region between two plateaus.[13,21,22] By contrast, at least up to the system sizes for which we have done the computation, it is observed that, from Figs. 2 and 3, sharp spikes of the fluctuations are obviously absent in our results. Instead, steps with rounded or flat tops or bottoms occur as we vary μ. This feature can be understood in terms of the total electrostatic potential energy changing slowly or even remaining constant for some finite interval of the chemical potential. It is also true that the systems we have studied show a relatively small number of conductance fluctuations as μ varies, compared with experiments. However, we should expect more fluctuations in a bigger system. Our model seems to show this behavior as the system size is increased. It is therefore not appropriate to analyze the distribution of conductance[13] from our results which only contain small numbers of independent conductance values.

Another important comparison is the temperature depen-

dence of the conductance fluctuations. Finite temperature reduces the amplitudes of the fluctuations because the fluctuation of the occupation number in each localized state is smoothed out by the finite thermal energy. In our model, it can be observed that the width of each fluctuation ''step'' does not vary with temperature (see Fig. 3). In experiments, data[22] demonstrate indeed that the amplitudes of peaks and dips are enhanced as the temperature is lowered. No obvious shrinking of their widths can be seen there.

We now come to the behavior of fluctuation peaks and dips at different magnetic fields. Although there is no explicit magnetic-field dependence in our model, we argue here, by noting that straight lines on the V_g-B plane[22] are obtained provided the system preserves the filling factor along each line, the occurrence of straight lines is consistent with the spirit of our model.

As mentioned in the Introduction, the slopes of two sets of lines are parallel to those associated with the centers of the neighboring plateaus. More explicitly, it is actually observed that each of these straight lines follows the equation $V_g = CB + D$ with C and D being constants. This behavior can be understood in terms of the physics of the Si MOSFET,[14] as has been discussed in Ref. 22. With the filling factor given by the relation $\nu = (V_g - V) \varepsilon \varepsilon_0 h / de^2 B$ as a perpendicular magnetic field B is applied, we have

$$V_g = \frac{e^2 d}{\varepsilon \varepsilon_0 h} \nu B + V. \qquad (4)$$

Here V is some constant and represents a threshold voltage, and d is a distance of the order of the thickness of the SiO$_2$ layer. To describe the ith straight line on the V_g-B plot, another constant V_i, for example, is needed. For different parallel lines on the V_g-B plane, we have different V_i's. Along each line, the filling factor and V_i are constants. This means that, as V_g and B are both varied along the line, the fluctuation peaks and dips evolve in such a way that the filling factor of the system is unchanged for a given fluctuation. More explicitly, the value of ν is observed to be either i or $i+1$ for the $(i+1)$th transition region, depending on which plateau region the lines belong to.

In our model, conductance fluctuations are associated with the occupancy of localized states in the 2DES. For the occupancy to fluctuate, the state must have energy near the chemical potential. Hence, along each straight line, which connects peaks or dips for different (V_g, B), the localized states are at the chemical potential. The fact that ν along the straight line is the same as i, for example, associated with the ith plateau center means that the localized states in both cases must have the same total (kinetic plus electrostatic) energy as the states in the ith Landau level. This is indeed

possible if the localized states belong to the Landau levels of the 2DES. Following this argument, as the chemical potential crosses the center of a disordered-broadened Landau level in the transition region, localized states at two tails of the Landau level then give the two slopes of straight lines corresponding to two different energies of the states at two plateau centers.

IV. CONCLUSIONS

In this paper, we have constructed a simple semiclassical model which produces conductance fluctuations in strong magnetic fields due to the Coulomb interaction between electrons. The inclusion of the long-range Coulomb interaction causes the occupation number in each localized state in the bulk to fluctuate as the chemical potential is varied. By taking into account the influence of the electrostatic potential between localized states and the saddle point, the energy of the saddle point in the potential affecting mobile electrons then also varies with the chemical potential. Through this saddle point, the conductance due to the transmission of edge states from one contact to the other thus fluctuates with the chemical potential. We study the model at finite temperature by numerical simulation using the Monte Carlo methods and exact enumeration. At low temperature, the Monte Carlo results suffer slow equilibration. Strong fluctuations due to the nonequilibration of the system in this case make it difficult to extract interaction-driven fluctuations. By contrast, results obtained using exact enumeration clearly exhibit significant fluctuations as a function of the chemical potential.

In comparing these results with the experiments, our model shows qualitatively consistent behaviors with the experiments as the gate voltage and the magnetic field are both varied. There are, however, some features that differ in our results and experiments. In particular, although our simulations indeed exhibit fluctuations depending on realizations of disorder, they give fluctuations which are like steps instead of the sharp peaks and dips observed in experiments. These discrepancies could arise because we have neglected interactions between bulk extended electrons and many specific details in the Si MOSFET.

*Present address: Department of Applied Physics, University of Tokyo, 7-3-1, Hongo, Bunkyo-ku, Tokyo 113, Japan.

[1] S. B. Kaplan and A. Hartstein, Phys. Rev. Lett. **56**, 2403 (1986); W. J. Skocpol, P. M. Mankiewich, R. E. Howard, L. D. Jackel, D. M. Tennant, and A. D. Stone, *ibid.* **56**, 2865 (1986).

[2] S. Washburn, IBM J. Res. Dev. **32**, 335 (1988); for a list of related references, see S. Das Sarma, T. Kawamura, and S. Washburn, Am. J. Phys. **63**, 683 (1995).

[3] P. A. Lee, A. D. Stone, and H. Fukuyama, Phys. Rev. B **35**, 1039 (1987); C. W. J. Beenakker and H. van Houten, in *Solid State Physics: Advances in Research and Applications*, edited by H. Ehrenreich and D. Turnbull (Academic Press, New York, 1991), Vol. 44.

[4] B. I. Halperin, Phys. Rev. B **25**, 2185 (1982).

[5] J. A. Simmons, S. W. Hwang, D. C. Tsui, H. P. Wei, L. W. Engel, and M. Shayegan, Phys. Rev. B **44**, 12 933 (1991).

[6] P. C. Main, A. K. Geim, H. A. Carmona, C. V. Brown, T. J. Foster, R. Taboryski, and P. E. Lindelof, Phys. Rev. B **50**, 4450 (1994).

[7] A. K. Geim, P. C. Main, P. H. Beton, L. Eaves, S. P. Beaumont, and C. D. W. Wilkinson, Phys. Rev. Lett. **69**, 1248 (1992); C. V. Brown, A. K. Geim, T. J. Foster, C. J. G. M. Langerak, and P. C. Main, Phys. Rev. B **47**, 10 935 (1993).

[8] A. Morgan, D. H. Cobden, M. Pepper, G. Jin, Y. S. Tang, and C. D. W. Wilkinson, Phys. Rev. B **50**, 12 187 (1994).

[9] J. K. Jain and S. A. Kivelson, Phys. Rev. Lett. **60**, 1542 (1988).

[10] J. M. Kinaret and P. A. Lee, Phys. Rev. B **43**, 3847 (1991).

[11] D.E. Khmel'nitskii and M. Yosefin, Physica A **200**, 525 (1993); Surf. Sci. **305**, 507 (1994); D. L. Maslov and D. Loss, Phys. Rev. Lett. **71**, 4222 (1993); S. Xiong, N. Read, and A. D. Stone, Phys. Rev. B **56**, 3982 (1997).

[12] B. Huckestein, Rev. Mod. Phys. **67**, 357 (1995).

[13] D. H. Cobden and E. Kogan, Phys. Rev. B **54**, R17 316 (1996).

[14] For general aspects of MOSFETs, see, for example, T. Ando, A. B. Fowler, and F. Stern, Rev. Mod. Phys. **54**, 437 (1982).

[15] T. Ando, Phys. Rev. B **49**, 4679 (1994).

[16] Z. Wang, B. Jovanović, and D.-H. Lee, Phys. Rev. Lett. **77**, 4426 (1996).

[17] S. Cho and M. P. A. Fisher, Phys. Rev. B **55**, 1637 (1996).

[18] B. Jovanović and Z. Wang, Phys. Rev. Lett. **81**, 2767 (1998).

[19] Y. Avishai, Y. Band, and D. Brown, cond-mat/9901328 (unpublished).

[20] A. G. Galstyan and M. E. Raikh, Phys. Rev. B **56**, 1422 (1997).

[21] D. H. Cobden, C. H. W. Barnes, C. J. B. Ford, J. T. Nicholls, and M. Pepper, in *Proceedings of the 24th ICPS*, edited by D. Gershoni (World Scientific, Singapore, 1999).

[22] D. H. Cobden, C. H. W. Barnes, and C. J. B. Ford, Phys. Rev. Lett. **82**, 4695 (1999); D. H. Cobden (private communication).

[23] H. A. Fertig and B. I. Halperin, Phys. Rev. B **36**, 7967 (1987); M. Büttiker, in *Semiconductors And Semimetals*, edited by M. Reed (Academic Press, San Diego, 1992), Vol. 35.

[24] M. Büttiker, Phys. Rev. B **41**, 7906 (1990).

[25] See discussions, for example, in P. A. Lee and T. V. Ramakrishnan, Rev. Mod. Phys. **57**, 287 (1985).

[26] A. L. Efros and B. I. Shklovskii, J. Phys. C **8**, L49 (1975); in *Electron-Electron Interaction in Disordered Systems*, edited by A. L. Efros and M. Pollak (North-Holland, Amsterdam, 1985).